

| | | | | | | | |
|------------------|----|------|-------|-------|------|------|------|
| H ₂ O | 18 | 1 | 0.409 | 0.375 | 1 | 1.56 | 1.63 |
| CO ₂ | 44 | 2.44 | 1 | 0.92 | 0.64 | 1 | 1.04 |
| O ₃ | 48 | 2.67 | 1.09 | 1 | 0.61 | 0.96 | 1 |

S2. Irradiance absorption by the canopy

Solar radiation is the key determinant of the productivity of any crop. The radiation absorbed (direct and diffuse) photosynthetically active radiation, PAR_{tot} (in W/m^2) by crops will have a direct impact on canopy photosynthesis (and associated stomatal conductance) and affect crop leaf phenology and hence net primary productivity (NPP). PAR absorbed by crops is divided into two categories, direct (PAR_{dir}) and diffuse (PAR_{diff}) radiation. PAR_{dir} is the PAR which reaches the crop leaf surface without being scattered, whereas PAR_{diff} can be naturally (by cloud cover and naturally occurring particles in the atmosphere) or artificially scattered (e.g. by pollutant aerosol). PAR can also be reflected by surfaces.

To estimate the total irradiance (PAR_{tot} which is equal to $PAR_{dir} + PAR_{diff}$) incident on sunlit and shaded parts of the canopy we use the method of (De Pury and Farquhar, 1997).

S2a. Total Photosynthetic Active Radiation (PAR_{tot})

PAR absorbed per unit leaf area is divided into PAR_{dir} , PAR_{diff} which also includes scattered (re-reflected by the canopy) beam calculated by,

$$PAR_{dir}(LAI) = (1 - \rho_{cb}(\beta)) K_b' I_b(0) \exp(-k_b' LAI) \quad [S1]$$

Where, $\rho_{cb}(\beta) = 1 - \exp\left[\frac{2\rho_h k_b}{1+k_b}\right]$ -eq.S2; K_b' is beam and scattered beam PAR extinction coefficient ; $I_b(0)$ is the initial beam irradiance, representing the intensity of direct sunlight before it interacts with the canopy

$$PAR_{diff}(LAI) = (1 - \rho_{cd}) k_d' I_d(0) \exp(-k_d' LAI) \quad [S3]$$

Where, $\rho_{cd} = \frac{1}{I_d(0)} \int_0^{\pi/2} N_d(\alpha) \rho_{cb}(\alpha) d\alpha$ -eq.[S4];

K_d' is diffuse and scattered diffuse PAR extinction coefficient

The total absorbed irradiance per unit leaf area is calculated as:

$$PAR_{total} = PAR_{dir}(LAI) + PAR_{diff}(LAI) \quad [S6]$$

Estimations of the direct, diffuse and scattered (re-reflected) irradiance are necessary to calculate the PAR incident on the sunlit (LAI_{sun}) and shaded (LAI_{shade}) portions of the canopy, which are then calculated based on the equations described below:

S2b. Total irradiance absorbed as shaded leaves ($I_{Ish}(LAI)$) per unit leaf area are calculated as ;

$$PAR_{sh}(LAI) = PAR_{diff}(LAI) + PAR_{bs}(LAI) \quad [S7]$$

where $PAR_{diff}(LAI)$ is diffuse irradiance (see eq.) and $PAR_{bs}(LAI)$, direct scattered beam (another form of diffuse radiation) is calculated as:

$$PAR_{bs}(LAI) = PAR_b(0) [PAR_{dir} - (1 - \sigma)k_b \exp(-k_b LAI)] \quad [S8]$$

S2c. Total irradiance absorbed by per unit leaf area of the sunlit leaf

$$PAR_{sun}(LAI, \beta) = PAR_{sh}(LAI) + PAR_{bsun}(\beta) \quad [S9]$$

Where; $PAR_{sh}(LAI)$ is irradiance absorbed by shaded leaves (see equation S7) and $PAR_{bsun}(\beta)$, beam irradiance absorbed by sunlit leaves and calculated as below:

$$PAR_{bsun}(\beta) = (1 - \sigma)I_b(0) \frac{\cos \alpha_l}{\sin \beta} \quad [S10]$$

S3. Solar elevation Angle

$\sin \beta$ which is defined as the solar elevation angle, varies over the course of the day as a function of latitude and day length as described in eq. 8, this eq. and the other solar geometry equations required for its calculation are taken from Campbell & Norman, (1998).

$$\sin \beta = \sin \lambda \cdot \sin \delta + \cos \lambda \cdot \cos \delta \cdot \cos hr \quad S11$$

where β is the solar elevation above the horizontal, λ is the latitude, δ is the angle between the sun's rays and the equatorial plane of the earth (solar declination), hr is the hour angle of the sun and is given by $[15(t-t_0)]$ where t is time and t_0 is the time at solar noon.

The solar declination (δ) is calculated according to eq. 9.

$$\delta = -23.4 \cos[360(td + 10)/365] \quad S12$$

where t_d is the year day.

The time, t is in hours (standard local time), ranging from 0 to 23. Solar noon (t_0) varies during the year by an amount that is given by the equation of time (e , in min) and calculated by:-

$$t_0 = 12 - LC - e \quad S13$$

where LC is the longitude correction. LC is +4 or -4 minutes for each degree you are either east or west of the standard meridian. e is a 15 to 20-minute correction, which depends on the year day according to eq. 11.

$$e = \frac{-104.7 \sin f + 596.2 \sin^2 f + 4.3 \sin^3 f - 12.7 \sin^4 f - 429.3 \cos f - 2.0 \cos^2 f + 19.3f}{3600}$$

where $f = 279.575 + 0.9856 t_d$ in degrees.

It is also necessary to calculate the day length so that the hour angle of the sun can be calculated throughout the day. Day length is defined as the number of hours that the sun is above the horizon and requires the hour angle of the sun, hr , at sunrise or sunset to be calculated with eq. S14.

$$\cos hr = -\tan \lambda \cdot \tan \delta \quad S14$$

so that day length in hours equals $2hr/15$.

Table S2. Variables and parameters used to calculate the multi-layer canopy irradiance after De Pury and Farquhar (1997).

| Parameters | Description | Value | Units |
|-------------------|--|------------------|--------------------------------------|
| K_b' | Beam and scattered beam PAR extinction coefficient | $0.46/\sin\beta$ | |
| K_d' | Diffuse and scattered diffuse PAR extinction coefficient | 0.719 | |
| ρ_{cb} | Canopy refection coefficient for beam PAR | | |
| ρ_{cd} | Canopy reflection coefficient for diffuse PAR | | |
| β | Solar elevation angle | | Radians |
| δ | Solar declination angle | | Radians |
| I_{lb} (LAI) | Absorbed beam plus scattered beam PAR per unit leaf area | | $\mu\text{mol m}^{-2} \text{s}^{-1}$ |
| I_{ld} (LAI) | Absorbed diffuse plus scattered diffuse PAR per unit leaf area | | $\mu\text{mol m}^{-2} \text{s}^{-1}$ |
| I_l (LAI) | Total absorbed PAR per unit leaf area | | $\mu\text{mol m}^{-2} \text{s}^{-1}$ |
| I_b (LAI) | Direct PAR per unit ground area | | $\mu\text{mol m}^{-2} \text{s}^{-1}$ |
| I_d (LAI) | Diffuse PAR per unit ground area | | $\mu\text{mol m}^{-2} \text{s}^{-1}$ |
| $I_d(0)$ | Diffuse PAR per unit ground area at the top of the canopy | | $\mu\text{mol m}^{-2} \text{s}^{-1}$ |
| $I_b(0)$ | Beam PAR per unit ground area at the top of the canopy | | $\mu\text{mol m}^{-2} \text{s}^{-1}$ |
| | | | |
| I_{lbb} (LAI) | Absorbed beam PAR without scattering per unit leaf area | | $\mu\text{mol m}^{-2} \text{s}^{-1}$ |
| I_{bs} (LAI) | Absorbed scattered beam PAR per unit leaf area | | $\mu\text{mol m}^{-2} \text{s}^{-1}$ |
| I_{lbsun} (LAI) | Beam PAR absorbed by sunlit leaves per unit leaf area | | $\mu\text{mol m}^{-2} \text{s}^{-1}$ |
| I_{lsh} (LAI) | Beam PAR absorbed byshaded leaves per unit leaf area | | $\mu\text{mol m}^{-2} \text{s}^{-1}$ |

| | | | |
|-----------------|--|------|-------------------------|
| I_{sun} (LAI) | Total PAR absorbed by sunlit leaves per unit leaf area | | $\mu mol m^{-2} s^{-1}$ |
| (LAI) | Cumulative leaf area index from top of canopy (L=0 at top) | | $m^2 m^{-2}$ |
| $f_{1,2}$ (LAI) | Fraction of leaf area in a leaf-angle class | | |
| f_{sh} (LAI) | Fraction of leaves that are shaded | | |
| f_{sun} (LAI) | Fraction of leaves that are sunlit | | |
| σ | Leaf scattering coefficient for PAR | 0.15 | |
| α_1 | Angle of beam irradiance to the leaf normal | 0.5 | Radians |

S4. Methodology for gap-filling and standardisation of data for AgMIP Ozone

This document describes the methodological approach that was applied in order to search for gaps and quality issues in time-series (gas concentration and meteorological) datasets, and the approach used for filling gaps.

Where gaps had already been filled by the team collecting the data then this interpolated data was left under the assumption that it would be a more accurate reflection of the experimental conditions.

Gap filling methodology for hourly data : During the data standardisation process some data gaps were identified. These ranged in size from a single hour of missing data, to several consecutive hours, to several consecutive days, weeks, or even months. A requirement of input data for modellers is that it is continuous; the following gap filling methodology was therefore devised. These gap filling methods are only applied for the duration of the plants growing season (i.e. between sowing and harvest):

Single hours of missing data were filled by taking the average of the hourly values coming the hour before, and the hour after, the missing value.

Several consecutive hours of missing data (23 hours or less) were filled by taking the average of the corresponding hour the day before, and the day after; and repeating this for each missing hour of data. If data were unavailable from that hour of the previous day, then only the value from the day after was used and vice versa. If there is no data available in either the day before or after, then the method is used (see below point 2.).

Gaps larger than 24 hours could be filled using the following methods:

1. Gaps between 24 hours and 168 hours (i.e. from 1 day up to 1 week) would be filled with the averages from that same hour of the equivalent day, the week before and the week after (i.e. averaging 2 numbers). If data were unavailable from those hours

of the previous week, then only the values from the week after would be used (and vice versa).

2. Gaps longer than 1 week would be filled with the diurnal averages from one week before and after the period of missing data (i.e. potentially averaging 14 hours of data, but in cases where data is sparse then it could only be a couple of hours). Gap filled values would not be used in calculating averages. Where data is daily, i.e. some meteorological data, the average of the 7 days before and/or after is used.

There were some instances where data gaps extended for several months. For these extensive gaps, the following methods were used:

- A. All datasets from Xiaoji, China, had about a 4-month gap in meteorological and ozone data at the start of the growing season. At this stage of the growing season, plants will either have not yet emerged or have a very small LAI and therefore any ozone uptake would have been minimal. Ozone gaps were filled with the diurnal averages of the first two weeks of the ambient experimental data for each year. Meteorological data was filled using Nasa Power data (<https://power.larc.nasa.gov/data-access-viewer/>). The variables selected are in the appendix below. In Xiaoji China, global radiation was measured, whereas the Nasa Power data platform only provides Photosynthetically Active Radiation (PAR). To convert global radiation to PAR, values were multiplied by two and divided by 24 to be comparable with global radiation in MJ/m²/hour.
- B. If the gap occurs before exposure data begins then the ambient or non-filtered treatment is gap filled using the above methodology and then this data is used for all treatments to ensure that concentrations are not overestimated. If there is no ambient treatment then averages of the treatment closest to ambient is used. If there are gaps in gas data after the beginning of exposure date, then averages from that treatment are used (as opposed to ambient). If no date for start of exposure is provided, then exposure is assumed to start when the gas data begins (even if it is na). Similarly, once exposure has ended then only averages from the period after exposure were used. If there was not enough data to base averages on then ambient data was used (Nottingham 1996).
- C. Any ozone values of less than 0 were treated as gaps and filled following the above methods, depending on the size of gap.
- D. If mean air temperature was not available but minimum and maximum air temperature was, the average of these two values was used and the source of the data was label 'c' for calculated.
- E. Sections of the dataset which had been gap filled were clearly identified using a categorisation system in an adjacent 'data source' column, so that these data could be identified at a later stage, and so that alternative measured or modelled data could be sought. The percentage of gap-filled data within the total time-series for each gas concentration and meteorological variable was also reported in the readme file accompanying each dataset.
- F. The Parameters downloaded from (<https://power.larc.nasa.gov/data-access-viewer/>)
- G. Hourly data was downloaded from the Nasa Power data access viewer for Xiaoji, China to fill gaps in meteorological data. The following parameters were selected: 1. Agroclimatology community; 2. Hourly; 3. Lat/long: 32.58333: 119.7; 4. Time extent: Determined by data gap in each year; 5. Format: CSV format; 6. Parameters: a) temp at 2m, b)relative humidity at 2m, c)wind speed at 2m, d) precipitation, e) radiation: "All Sky Surface photosynthetically active radiation" (PAR Total) (MJ/m²/day). This was converted to hourly global radiation (MJ/m²/h) by dividing to 24 and multiplying with 2 because PAR ~ 0.5 * global radiation

S4. O₃ Resistance

Atmospheric Resistance

$$r_a = \frac{1}{K u^*} \left(\log \left(\frac{z_2}{z_1} \right) - \Psi_h \left(\frac{z_2}{L} \right) + \Psi_h \left(\frac{z_1}{L} \right) \right)$$

u^* Friction velocity m/s

K Von Karman's constant

L Monin-Obukhov length m

z_1 Lower height m

z_2 Upper height m

Ψ_h Flux-gradient stability function for heat

Heat flux

$$\Psi_h(x) = \begin{cases} 2 \log \left(\frac{1 + \sqrt{1 - 16x}}{2} \right) & x < 0 \\ -5x & x \geq 0 \end{cases}$$

Quasi-laminar boundary layer resistance

$$r_{b,o3} = \frac{2}{K u^*} \left(\frac{\left(\frac{V}{diff} \right)}{PR} \right)^{\frac{2}{3}}$$

u^* Friction velocity m/s

K Von Karman's constant

V Kinematic viscosity of air at 20°C m²/s

$diff$ Molecular diffusivity in air m²/s

PR Prandtl number

In-canopy resistance

$$r_{inc} = 14 \frac{SAI h}{u^*}$$

External plant cuticle resistance

$$r_{ext} = \frac{2500}{SAI}$$

Stomatal resistance

$$r_{sto} = \min\left(100000, \frac{41000}{g_{sto}}\right)$$

Surface resistance per layer

$$r_c = \begin{cases} r_b + \frac{1}{\left(\frac{1}{r_{sto}} + \frac{1}{r_{ext}}\right)} & LAI > 0 \\ r_b + r_{ext} & SAI > 0 \end{cases}$$

S5. The timing of crop emergence, anthesis and harvest

Fig S1. The Chinese FACE-O3 dataset were used to plot modelled phenological stages against experimental dataset for the year a) 2008 (training set) and b) 2007 and 2009 (testing set)

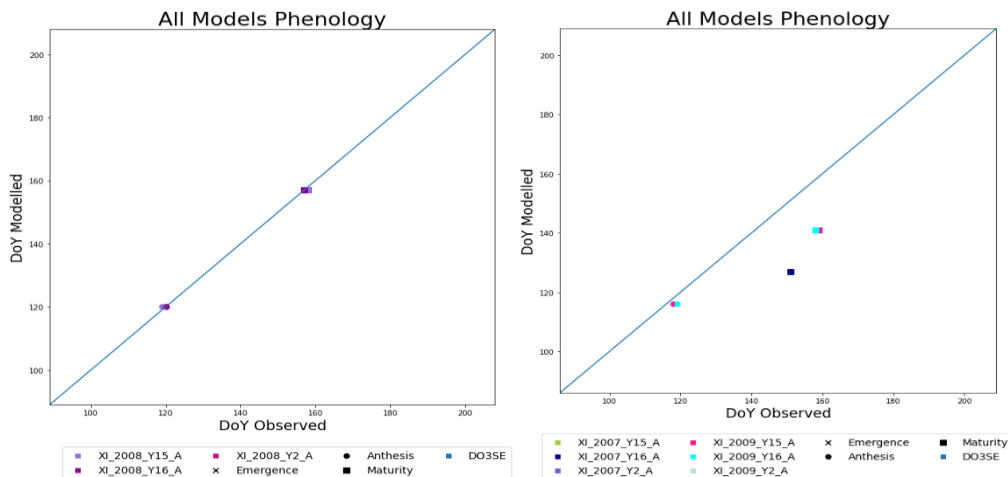


Fig S2. The Chinese FACE-O3 dataset were used to plot modelled grain dry matter (g/m^2) against experimental dataset for the year 2008 for tolerant (Y16) and sensitive cultivar (Y2) (training set)

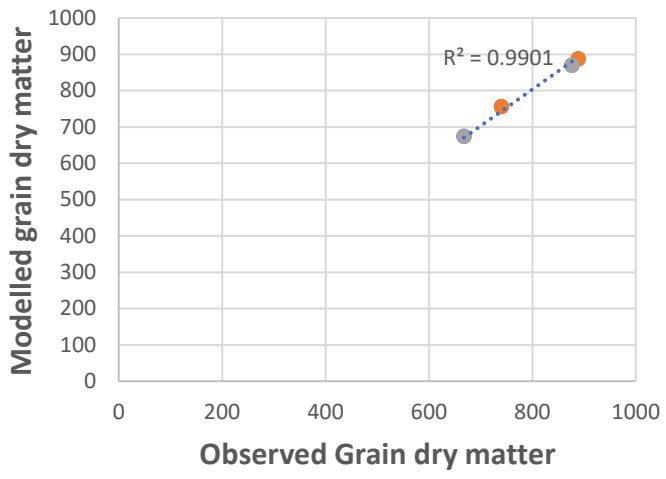


Table S3. DO₃SE-Crop variables

| Variable | Unit | Description |
|------------------|--|--|
| T_{eff} | °C days | Effective temperature accumulated between sowing to maturity |
| DVI | - | Development index |
| T_{air} | °C | Surface air temperature in degrees Celsius |
| $T_{air,k}$ | degrees Kelvin | Surface air temperature in Kelvin |
| T_{min} | °C | Daily minimum surface air temperature |
| T_{max} | °C | Daily maximum surface air temperature |
| V_{dd} | days | Accumulated vernalised days |
| V | days | Vernalised days |
| V_d | days | Devernalised days |
| VF | - | Vernalisation factor |
| PP | hrs | Photoperiod |
| PF | - | Photoperiod factor |
| A_{net} | $\mu\text{mol CO}_2 \text{ m}^{-2} \text{ s}^{-1}$ | Net photosynthesis or rate of CO ₂ assimilation |
| A_c | $\mu\text{mol CO}_2 \text{ m}^{-2} \text{ s}^{-1}$ | RuBP (ribulose-1,5-bisphosphate) limited A_{net} |
| A_j | $\mu\text{mol CO}_2 \text{ m}^{-2} \text{ s}^{-1}$ | Electron transport limited A_{net} |
| A_p | $\mu\text{mol CO}_2 \text{ m}^{-2} \text{ s}^{-1}$ | TPU (triose phosphate) limited A_{net} |
| R_d | $\mu\text{mol CO}_2 \text{ m}^{-2} \text{ s}^{-1}$ | Dark respiration |
| f_{sw} | - | Plant available soil water stress factor |
| ASW | m^3/m^3 | Plant available soil water |
| C_i | $\mu\text{mol}/\text{mol}$ | Intercellular CO ₂ partial pressure |
| O_i | mmol/mol | Intercellular O ₂ concentrations |
| Γ^* | $\mu\text{mol}/\text{mol}$ | CO ₂ compensation point in the absence of respiration |
| Γ | $\mu\text{mol}/\text{mol}$ | CO ₂ compensation point |
| J | $\mu\text{mol CO}_2 \text{ m}^{-2} \text{ s}^{-1}$ | electron transport rate |
| VPD | kPa | Leaf to air vapour pressure deficit |
| f_{st} | $\text{nmol O}_3 \text{ m}^{-2} \text{ s}^{-1}$ | Leaf level stomatal O ₃ flux |
| $accf_{st}$ | $\text{mmol O}_3 \text{ m}^{-2}$ | Accumulated stomatal O ₃ flux |
| $f_{O_3,s}(d)$ | - | Effect of daily cumulative stomatal O ₃ flux on $V_{C_{max}}$ |
| $f_{O_3,s}(h)$ | - | Effect of hourly cumulative stomatal O ₃ flux on $V_{C_{max}}$ |
| $f_{O_3,s}(d-1)$ | - | Previous days effect of cumulative stomatal O ₃ flux on $V_{C_{max}}$ |
| $r_{O_3,s}$ | - | Incomplete overnight recovery of O ₃ affected $V_{C_{max}}$ |
| f_{LA} | - | Leaf age related capacity to recover from accumulated stomatal O ₃ flux |
| $f_{O_3,l}$ | - | Weighted accumulated stomatal O ₃ flux that determines the onset of leaf senescence |
| f_{LS} | - | Accumulated stomatal O ₃ flux effect on leaf senescence |
| tl | °C days | Effective temperature accumulated by a leaf after emergence ($DVI = 0$) |

| | | |
|----------------|--|--|
| tl_{ep} | - | Effective temperature accumulated by a leaf between full expansion and the onset of leaf senescence |
| tl_{epO_3} | - | Effective temperature accumulated by a leaf between full expansion and the onset of leaf senescence brought forward by O_3 |
| tl_{se} | - | Effective temperature accumulated by a leaf between the onset of leaf senescence and maturity |
| tl_{seO_3} | - | Effective temperature accumulated by a leaf between the onset of leaf senescence and maturity brought forward by O_3 |
| g_{CO_2} | $\mu\text{mol CO}_2 \text{ PLA m}^{-2} \text{ s}^{-1}$ | Stomatal conductance to CO_2 |
| f_{VPD} | - | Relationship between VPD and relative stomatal conductance |
| c_s | $\text{mol CO}_2/\text{mol}$ | Leaf surface CO_2 concentration |
| c_s | $\text{mol CO}_2/\text{mol}$ | Quasi laminar boundary layer surface CO_2 concentration |
| g_{bCO_2} | $\text{mol m}^{-2} \text{ s}^{-1}$ | Quasi laminar boundary layer conductance to CO_2 |
| C_z | $\text{nmol O}_3 \text{ m}^{-3}$ | O_3 concentration at reference height (z) |
| C_l | $\text{nmol O}_3 \text{ m}^{-3}$ | O_3 concentration at the upper surface of the laminar layer of a leaf |
| g_{O_3} | $\text{mmol O}_3 \text{ PLA m}^{-2} \text{ s}^{-1}$ | Stomatal conductance to O_3 (in $\text{mmol O}_3 \text{ m}^{-2} \text{ s}^{-1}$) |
| $g_{O_3m/s}$ | m/s | Stomatal conductance to O_3 (in m/s) |
| r_c | s/m | Leaf surface resistance to O_3 |
| r_{b,O_3} | s/m | Quasi laminar leaf boundary layer resistance to O_3 |
| r_a | s/m | Atmospheric resistance to O_3 |
| r_{inc} | s/m | In-canopy resistance to O_3 |
| r_{ext} | s/m | External plant cuticle resistance to O_3 |
| r_{sto} | s/m | Stomatal resistance to O_3 |
| u_z | m/s | Wind speed at a reference height z |
| u_l | m/s | Wind speed at the upper surface of the laminar layer of a leaf |
| LAI | $\text{m}^2 \text{ m}^{-2}$ | Leaf Area Index |
| $PAR_{dir,i}$ | W/m^2 | Direct PAR in canopy layer i |
| $PAR_{diff,i}$ | W/m^2 | Diffuse PAR in canopy layer i |
| PAR_{total} | W/m^2 | Direct and diffuse PAR at the top of the canopy |
| NPP | kg C m^{-2} | Net primary productivity |
| GPP | kg C m^{-2} | Gross primary productivity |
| R_p | kg C m^{-2} | Plant respiration |
| R_{pm} | kg C m^{-2} | Plant maintenance respiration |
| R_{pg} | kg C m^{-2} | Plant growth respiration |
| A_{netc} | kg C m^{-2} | Canopy net photosynthesis |
| R_{dc} | kg C m^{-2} | Non-water stressed canopy dark respiration |
| $f_{sw}R_{dc}$ | kg C m^{-2} | Water stressed modified canopy dark respiration |
| C_{root} | kg C m^{-2} | Root C pool |

| | | |
|------------------|---------------------------------|--------------------------------------|
| C_{leaf} | kg C m ⁻² | Leaf C pool |
| C_{stem} | kg C m ⁻² | Stem C pool |
| C_{resv} | kg C m ⁻² | Reserve C pool |
| C_{harv} | kg C m ⁻² | Harvest pool |
| P_{root} | - | Root C pool partition coefficient |
| P_{leaf} | - | Leaf C pool partition coefficient |
| P_{stem} | - | Stem C pool partition coefficient |
| P_{resv} | - | Reserve C pool partition coefficient |
| P_{harv} | - | Harvest C pool partition coefficient |
| $C_{leaf,green}$ | kg C m ⁻² | Green leaf C |
| $C_{leaf,brown}$ | kg C m ⁻² | Brown leaf C |
| SLA | m ² kg ⁻¹ | Specific Leaf Area |
| h | m | Crop height |
| $Yield_{grain}$ | g C m ⁻² | Grain yield |

Table S4. DO₃SE-Crop parameters for wheat. Highlighted are the parameters (and their associated ranges) which require calibration when applying DO₃SE-Crop to varying environmental conditions.

| Parameter | Unit | Default Value | Description | Reference | Range | Calibrated Parameter Value |
|-------------|--|---------------|--|--|---------|----------------------------|
| T_b | °C | 0 | Base temperature | (Tao, Zhang and Zhang, 2012; Osborne <i>et al.</i> , 2015) | -0.5-3 | -0.25 |
| T_o | °C | 20 | Optimum temperature | (Tao, Zhang and Zhang, 2012; Osborne <i>et al.</i> , 2015) | | 17.79 |
| T_m | °C | 30 | Maximum temperature | (Tao, Zhang and Zhang, 2012; Osborne <i>et al.</i> , 2015) | | 23.87 |
| TT_{emr} | °C d | 100 | Thermal time between sowing and emergence | (Lu <i>et al.</i> , 2018; Luo <i>et al.</i> , 2020) | | 220.6 |
| TT_{veg} | °C d | 940 | Thermal time between emergence and anthesis | Xiaoji experimental dataset | 400-940 | 940 |
| TT_{rep} | °C d | 304 | Thermal time between anthesis and maturity | (Wang <i>et al.</i> , 2013a); Xiaoji experimental dataset | 300-650 | 304 |
| PIV | | 1.5 | Vernalisation coefficient | (Tao, Zhang and Zhang, 2012; Wang <i>et al.</i> , 2013) | 2.9-4 | 2.9 |
| PID | | 40 | Photoperiod coefficient | (Wang <i>et al.</i> , 2013; Liu <i>et al.</i> , 2016; Zhao <i>et al.</i> , 2020) | 40-57 | 40 |
| VT_{max} | °C | 30 | Maximum daily temperature for vernalisation | Zheng <i>et al.</i> , 2015 | | |
| VT_{min} | °C | 15 | Minimum daily temperature for vernalisation | Zheng <i>et al.</i> , 2015 | | |
| ASW_{max} | m ³ /m ³ | 50 | Plant available soil water below which stomatal conductance will start to reduce | | | |
| ASW_{min} | m ³ /m ³ | 0 | Plant available soil water at which stomatal conductance will equal f_{min} | | | |
| V_{cmax} | μmol CO ₂ m ⁻² s ⁻¹ | 90 | Maximum carboxylation capacity at 25°C | (Büker <i>et al.</i> , 2012) | 90-140 | 137 |
| J_{max} | μmol CO ₂ m ⁻² s ⁻¹ | 180 | Maximum rate of electron transport at 25°C | (Büker <i>et al.</i> , 2012) | 180-250 | 228 |
| K_c | μmol/mol | 404.9 | Rubisco Michaelis-Menten constants for CO ₂ | (Medlyn <i>et al.</i> , 2002) | | |

| | | | | | | |
|-----------------|---|---------------------|--|---|-----------------|---------|
| K_0 | mmol/mol | 278.4 | Rubisco Michaelis-Menten constants for O ₂ | (Medlyn <i>et al.</i> , 2002) | | |
| Γ^* | $\mu\text{mol/mol}$ | 42.75 | CO ₂ compensation point in the absence of respiration | (Medlyn <i>et al.</i> , 2002) | | |
| a | - | 4 | Electron requirement for the formation of NADPH | (Sharkey <i>et al.</i> , 2007) | | |
| b | - | 8 | Electron requirement for the formation of ATP | (Sharkey <i>et al.</i> , 2007) | | |
| R_{dcoeff} | - | 0.015 | Leaf dark respiration coefficient | (Clark <i>et al.</i> , 2011) | 0.01-0.03 | |
| f_{min} | $\mu\text{mol CO}_2/\text{m}^2/\text{s}$ | 1000 | Minimum daytime stomatal conductance to CO ₂ | (Ewert and Porter, 2000) | | |
| m | - | 7 | composite sensitivity slope constant | (Büker <i>et al.</i> , 2012) | 4-15 | 5 |
| VPD_0 | kPa | 2.2 | stomatal conductance sensitivity to VPD | UNECE, 2017; Pande <i>et al.</i> sub | | |
| γ_1 | - | 0.027 | O ₃ short-term damage co-efficient | (Ewert and Porter, 2000) | | |
| γ_2 | $(\text{nmol O}_3 \text{ m}^{-2} \text{ s}^{-1})^{-1}$ | 0.0045 | O ₃ short-term damage co-efficient | (Ewert and Porter, 2000) | | |
| γ_3 | $(\mu\text{mol O}_3 \text{ m}^{-2})^{-1}$ | 0.00005 | O ₃ long-term damage co-efficient | (Ewert and Porter, 2000) | 0.00001-0.00009 | 0.00002 |
| γ_4 | - | | O ₃ long-term damage co-efficient determining onset of senescence | | 1-6 | 5 |
| γ_5 | - | | O ₃ long-term damage co-efficient determining maturity | | 0.2-0.5 | 0.4 |
| $CLsO3$ | $\text{mmol O}_3 \text{ m}^{-2}$ | 12.9,22.5 | Critical accumulated stomatal O ₃ flux that determines the onset of leaf senescence | (Osborne <i>et al.</i> , 2019; Feng <i>et al.</i> , 2022) | 12.9-22.5 | 13.5 |
| r_{ext} | m/s | 2500 | External leaf cuticular resistance to O ₃ uptake | UNECE, 2017 | | |
| L | m | 0.02 | Cross wind leaf dimension for wheat | UNECE, 2017 | | |
| P_{st} | Pa | 1.013×10^5 | Standard air pressure at 20°C | UNECE, 2017 | | |
| T_{st} | °C | 20 | Standard temperature | UNECE, 2017 | | |
| R | J/mol/K | 8.31447 | Universal gas constant | UNECE, 2017 | | |
| n_e | $\text{mol CO}_2 \text{ m}^{-2} \text{ s}^{-1} \text{ kg C} (\text{kg N})^{-1}$ | 0.0008 | Constant relating leaf nitrogen to rubisco carboxylation capacity | (Clark <i>et al.</i> , 2011) | | |
| n_0 | $\text{kg N}[\text{kg C}]^{-1}$ | 0.073 | Top canopy leaf N concentration | (Clark <i>et al.</i> , 2011) | | |
| kN | | 0.78 | Nitrogen profile co-efficient | (Clark <i>et al.</i> , 2011) | | |
| R_{gcoeff} | - | 0.25 | Plant growth respiration coefficient | (Osborne <i>et al.</i> , 2015) | 0.15-0.25 | 0.16 |
| α_{root} | - | 18.5 | Coefficient for determining partitioning | (Osborne <i>et al.</i> , 2015) | 16-19 | 18.4 |
| α_{stem} | - | 16.0 | Coefficient for determining partitioning | (Osborne <i>et al.</i> , 2015) | 16-17 | 16.8 |

| | | | | | | |
|-----------------|------------------|---------|--|---|----------|--------|
| α_{leaf} | - | 18.0 | Coefficient for determining partitioning | (Osborne <i>et al.</i> , 2015) | 18-19 | 18.4 |
| β_{root} | -- | -20.0 | Coefficient for determining partitioning | (Osborne <i>et al.</i> , 2015) | 20-21 | -20.9 |
| β_{stem} | - | -15.0 | Coefficient for determining partitioning | (Osborne <i>et al.</i> , 2015) | 14-16 | -14.5 |
| β_{leaf} | - | -18.5 | Coefficient for determining partitioning | (Osborne <i>et al.</i> , 2015) | 18-19 | -18.11 |
| f_c | - | 0.5 | Carbon fraction of dry matter | (Osborne <i>et al.</i> , 2015) | | |
| Υ | $m^{-2} kg^{-1}$ | 27.3 | Coefficient for determining specific leaf area | (Osborne <i>et al.</i> , 2015) | 14-28 | 15 |
| δ | - | -0.0507 | Coefficient for determining specific leaf area | (Osborne <i>et al.</i> , 2015) | | |
| k | - | 1.4 | allometric coefficient which relates C_{stem} to h | (Osborne <i>et al.</i> , 2015) | | |
| τ | - | 0.4 | allometric coefficient which relates C_{stem} to h | (Osborne <i>et al.</i> , 2015) | 0.3-0.6 | 0.5 |
| D_w | - | 1/0.84 | Conversion factor to allow for grain moisture content | (Mulvaney and Devkota, 2020) | | |
| E_g | - | 0.85 | Conversion factor for grain to ear ratio | (Nagarajan <i>et al.</i> , 1999; Kutman, Yildiz and Cakmak, 2011) | 0.7-0.85 | 0.85 |

Table S5. DO₃SE-crop phenology parameters description and relation to the thermal time

| Paramter | Description | % of thermal time, from start of growing season |
|--|--|---|
| $f_{tl,em}^a$ | Crop emergence (DVI=0 ^b), end of TT _{emr} ^b | 5 |
| $f_{tl,ma}^a$ | Start of anthesis to maturity ^a , $f_{tl,ep}^a + f_{tl,se}^a$ | 50 |
| $f_{tl,ep}^a$ | Start of anthesis ^a (DVI=1 ^b) to flag leaf senescence ^a , flag leaf fully developed ^a , start of TTrep ^b | 34 |
| $f_{tl,se}^a$ | Start of flag leaf senescence to harvest(DVI=2 ^b) | 16 |
| Mid-anthesis, start of fphen_3_ETS, start of fphen_4_ETS | Half way through flowering | 8 |

^a(Ewert and Porter, 2000), ^b(Osborne *et al.*, 2015), ^cMapping manual,2007

References :

- Campbell, G.S., Norman, J. M. (1998). *An introduction to Environmental Biophysics*. Second. Springer.
- De Pury, D. G. G. and Farquhar, G. D. (1997). Simple scaling of photosynthesis from leaves to canopies without the errors of big-leaf models. *Plant, Cell and Environment*, 20 (5), Blackwell Publishing Ltd., pp.537–557. [Online]. Available at: doi:10.1111/j.1365-3040.1997.00094.x [Accessed 21 September 2020].
- Büker, P. *et al.* (2012) 'DO 3SE modelling of soil moisture to determine ozone flux to forest trees', *Atmospheric Chemistry and Physics*, 12(12), pp. 5537–5562. doi: 10.5194/acp-12-5537-2012.
- Clark, D. B. *et al.* (2011) 'The Joint UK Land Environment Simulator (JULES), model description – Part 2: Carbon fluxes and vegetation dynamics', *Geoscientific Model Development*, 4(3), pp. 701–722. doi: 10.5194/gmd-4-701-2011.
- Ewert, F. and Porter, J. R. (2000) 'Ozone effects on wheat in relation to CO₂: Modelling short-term and long-term responses of leaf photosynthesis and leaf duration', *Global Change Biology*, 6(7), pp. 735–750. doi: 10.1046/j.1365-2486.2000.00351.x.
- Feng, Y. *et al.* (2022) 'Identifying and modelling key physiological traits that confer tolerance or sensitivity to ozone in winter wheat', *Environmental Pollution*. Elsevier Ltd, 304(April), p. 119251. doi: 10.1016/j.envpol.2022.119251.
- Liu, B. *et al.* (2016) 'Testing the responses of four wheat crop models to heat stress at anthesis and grain filling', *Global Change Biology*. John Wiley & Sons, Ltd, 22(5), pp. 1890–1903. doi: 10.1111/GCB.13212.
- Lu, X. *et al.* (2018) 'Lower tropospheric ozone over India and its linkage to the South Asian monsoon', *Atmospheric Chemistry and Physics*, 18(5), pp. 3101–3118. doi: 10.5194/acp-18-3101-2018.
- Luo, Y. *et al.* (2020) 'ChinaCropPhen1km: a high-resolution crop phenological dataset for three staple crops in China during 2000-2015 based on leaf area index (LAI) products', *Earth System Science Data*. Copernicus GmbH, 12(1), pp. 197–214. doi: 10.5194/ESSD-12-197-2020.
- Medlyn, B. E. *et al.* (2002) 'Temperature response of parameters of a biochemically based model of photosynthesis. II. A review of experimental data', *Plant, Cell and Environment*, 25(9), pp. 1167–1179. doi: 10.1046/j.1365-3040.2002.00891.x.
- Mulvaney, M. J. and Devkota, P. J. (2020) 'Adjusting Crop Yield to a Standard Moisture Content', *EDIS*. University of Florida George A Smathers Libraries, 2020(3). doi: 10.32473/EDIS-AG442-2020.
- Osborne, S. *et al.* (2019) 'New insights into leaf physiological responses to ozone for use in crop Modelling', *Plants*, 8(4). doi: 10.3390/plants8040084.
- Osborne, T. *et al.* (2015) 'JULES-crop: A parametrisation of crops in the Joint UK Land Environment Simulator', *Geoscientific Model Development*, 8(4), pp. 1139–1155. doi: 10.5194/gmd-8-1139-2015.
- Sharkey, T. D. *et al.* (2007) 'Fitting photosynthetic carbon dioxide response curves for C₃ leaves', *Plant, Cell and Environment*, 30(9), pp. 1035–1040. doi: 10.1111/j.1365-3040.2007.01710.x.
- Tao, F., Zhang, S. and Zhang, Z. (2012) 'Spatiotemporal changes of wheat phenology in China under the effects of temperature, day length and cultivar thermal characteristics', *European Journal of Agronomy*. Elsevier B.V., 43, pp. 201–212. doi: 10.1016/j.eja.2012.07.005.
- Wang, J. *et al.* (2013) 'Phenological trends of winter wheat in response to varietal and temperature

changes in the North China Plain', *Field Crops Research*. Elsevier B.V., 144, pp. 135–144. doi: 10.1016/j.fcr.2012.12.020.

Zhao, H. *et al.* (2020) 'Evaluating the effects of surface O₃ on three main food crops across China during 2015–2018', *Environmental Pollution*. Elsevier Ltd, 258. doi: 10.1016/J.ENVPOL.2019.113794.